Development 122, 3023-3033 (1996)
Printed in Great Britain © The Company of Biologists Limited 1996
DEV2070

Spatial and temporal patterns of c-*kit*-expressing cells in W^{lacZ}/+ and W^{lacZ}/W^{lacZ} mouse embryos

Florence Bernex[1], Paulo De Sepulveda[1], Chantal Kress[2], Colette Elbaz[1], Claude Delouis[1] and Jean-Jacques Panthier[1,*]

[1]URA-INRA de Génétique Moléculaire, Ecole Nationale Vétérinaire d'Alfort, 7 avenue du Général-de-Gaulle, 94704 Maisons-Alfort cedex, France
[2]Unité de Génétique des Mammifères, Institut Pasteur, 25 rue du Docteur Roux, 75724 Paris cedex 15, France

*Author for correspondence (e-mail address: panthier@jouy.inra.fr)

SUMMARY

In the mouse, the Kit receptor and its ligand, the stem cell factor (SCF), are encoded at the *W*/Kit and *Steel* loci, respectively. The Kit/SCF transduction pathway is involved in promoting cellular migration, proliferation and/or survival of melanoblasts, hematopoietic progenitors and primordial germ cells. Furthermore, a functional Kit/SCF pathway is required for the development of interstitial cells of Cajal (ICC) in the small intestine. Whereas all c-*kit*-expressing cells in embryogenesis were not identified, previous studies clearly demonstrated that the c-*kit* expression pattern extends well beyond cells known to be affected by *W* mutations. To investigate further Kit function, we specifically marked the c-*kit*-expressing cells and followed their fate during embryogenesis. A mutation was introduced by gene targeting at the *W/Kit* locus in mouse embryonic stem cells. The *lacZ* reporter gene was inserted into the first exon of c-*kit*, thus creating a null allele, called W^{lacZ}.

The *lacZ* expression reflects normal expression of the c-*kit* gene in W^{lacZ}/+ embryos. The comparison of the patterns of *lacZ*-expressing cells between W^{lacZ}/+ and W^{lacZ}/W^{lacZ} embryos allowed us to detect where and when melanoblasts, primordial germ cells and hematopoietic progenitors failed to survive in the absence of Kit. We also observed that ICC express c-*kit* during embryogenesis. ICC are found identically in W^{lacZ}/+ and W^{lacZ}/W^{lacZ} embryos. Therefore, ICC do not depend on Kit expression during embryogenesis. These results indicate that the function of the c-*kit* gene is only required for the postnatal development of the ICC.

Unexpected sites of c-*kit* expression were uncovered in embryos, including endothelial, epithelial and endocrine cells. None of these cells are dependent on Kit expression for their migration, proliferation and/or survival during embryogenesis. Nevertheless, we assume that the Kit/SCF pathway could be involved in the growth of transformed endothelial, epithelial and endocrine cells.

Key words: homologous recombination, ES cells, *W* locus, c-*kit* proto-oncogene, stem cell factor, receptor tyrosine kinase, mouse

INTRODUCTION

The c-*kit* proto-oncogene encodes Kit, the receptor tyrosine kinase for stem cell factor (SCF). In the mouse, c-*kit* is allelic with the *W*/*Kit* locus, and SCF is encoded at the *Steel (Sl)* locus (for review, see Galli et al., 1994; Witte, 1990). Because of the receptor-ligand relationship, both *W* and *Sl* mutant phenotypes are characterized by similar pleiotropic effects affecting three cellular lineages during embryogenesis. In the absence of Kit, migration, proliferation and/or survival are impaired in primordial germ cells (PGC) from E9.5 onwards, in melanoblasts from E11 onwards, and in hematopoietic precursors from E11-E12 onwards (Buehr et al., 1993; Mintz and Russell, 1957; Cable et al., 1995; Russell et al., 1968). As a result of the absence of hematopoietic erythroid cells, newborn mutant homozygotes die of anemia.

We hypothesized that anemia and the resulting death could mask the existence of other cellular lineages, which would be dependent on the Kit/SCF system. It is notable that northern and RNA in situ hybridization studies showed that c-*kit* and *Steel* are expressed in several other organs, such as the embryonic lung, kidney, gut and brain (Orr-Urtreger et al., 1990; Keshet et al., 1991; Matsui et al., 1990). Moreover, hybridization studies on *W* and *Sl* mutant embryos revealed that both c-*kit* and *Steel* are contiguously expressed in a wide variety of anatomical sites (Motro et al., 1991). The hypothesis that the Kit/SCF pathway may play a role at some of these sites is supported by the report that the interstitial cells of Cajal (ICC), considered to be responsible for the pacemaker activity of the intestine, express c-*kit* and are absent in the ileum of W/W^V adult mice. Despite the absence of notable morphological abnormalities, these mice display irregular patterns of electrical activity in the small intestine (Huizinga et al., 1995).

To identify other Kit-dependent cellular lineages during embryogenesis, we generated a null *W* mutant mouse using gene targeting. In the W^{lacZ} mutation, the c-*kit* gene was inactivated and replaced by the *Escherichia coli lacZ* gene. A nuclear localisation signal sequence fused to the *lacZ* gene

allowed an unambiguous blue staining of the nuclear membrane. As the *lacZ* expression in W^{lacZ}/+ embryos recapitulates the known Kit expression, we compared the spatial and temporal expression patterns of the *lacZ* gene in W^{lacZ}/+ and W^{lacZ}/W^{lacZ} embryos. The identity of Kit-positive cells was assessed, and sites of Kit expression were uncovered. Two types of β-galactosidase (β-gal)-positive cells were identified. (1) β-gal-positive cells of heterozygous embryos absent in homozygous mutants: among these cells, which depend on Kit for their migration, proliferation and survival, only melanoblasts, PGC and hematopoietic progenitors were identified. (2) β-gal-positive cells found at identical sites and stages of development in W^{lacZ}/+ and W^{lacZ}/W^{lacZ} embryos: these Kit-expressing cells, including endothelial cells and various endocrine cells, do not require Kit function. Interestingly, ICC were present in W^{lacZ}/W^{lacZ} newborn mice and thus do not depend on Kit for their migration, proliferation and/or survival during embryogenesis.

MATERIALS AND METHODS

Construction of the targeting replacement vector pGNΔ-Kit

The pGNΔ-Kit plasmid targeting vector was prepared from 129/Sv strain mouse DNA. To construct the plasmid, a single ligation involving three restriction fragments was conducted with (1) the 3486 bp *Sac*II-*Xho*I fragment (position 2497-5983) from pGN vector (Le Mouellic et al., 1990); (2) the 5.5 kb *Bgl*II-*Xba*I fragment from pPROKit/lacZ, containing successively 1.2 kb of c-*kit* 5′ flanking sequences together with the 5′-untranslated region and the first 18 coding nucleotides of c-*kit* exon 1, the *E. coli lacZ* gene containing the SV40 nuclear localisation signal (nls), the *neo* gene and a SV40 polyadenylation site (De Sepulveda et al., 1995), after the addition of *Xho*I and *Kpn*I linkers at *Xba*I and *Bgl*II sites respectively; and (3) the 6.1 kb *Sac*II-*Kpn*I fragment from cosmid pCOS.F, corresponding to the c-*kit* 3′ flanking sequences and containing the 5′ end of the c-*kit* first intron after filling-in the internal *Not*I site (De Sepulveda et al., 1995).

Embryonic stem cell culture, detection of homologous recombinants and generation of chimeric mice

A new line of embryonic stem (ES) cells, CK35, was established from a 129/Sv male embryo. CK35 ES cells were cultured on feeder layers of G418^r embryonic fibroblasts with ES medium. The *Not*I linearized pGNΔ-KIT plasmid was electroporated as previously described (Colucci-Guyon et al., 1994). DNA from surviving colonies was digested with *Eco*RI, and screened by Southern blotting using a 300 bp *Alu*I probe. Homologous recombinant clones contained a wild-type band (9.1 kb) and a mutant band (6.4 kb). Correct targeting was confirmed following a *Eco*RI/*Eco*RV digestion, which gave a wild-type (9.1 kb) band and a mutant (4 kb) one. Germ line transmission of the mutation was determined by Southern blot analysis.

RNA extraction and RT-PCR

Total RNA was extracted from livers of E15.5 and E16.5 embryos. c-*kit* mRNA was amplified using specific oligonucleotides K3 and K6 (Reith et al., 1990). The RT-PCR reaction was done as previously described (De Sepulveda et al., 1994).

Histology, β-gal activity detection and histochemical detection of PGC

Noon of the day of the plug was considered E0.5. Post-implantation embryos were recovered, rinsed in cold phosphate-buffered saline (PBS), fixed for 30 to 90 minutes, depending on their developmental stage, in PBS containing 4% paraformaldehyde (PFA) at 4°C. The embryos were rinsed twice in PBS and stained overnight in X-Gal buffer (0.4 mg/ml 5-bromo-4-chloro-3-indolyl-D-galactoside, 2 mM potassium ferricyanide, 2 mM potassium ferrocyanide and 4 mM $MgCl_2$ in PBS) at 32°C. Early stage embryos (E7-E10), once post-fixed in 4% PFA for at least two days, were first embedded in gelose and then in paraffin. For more advanced stages (from E11 onwards), embryos were frozen in Tissue Tek (OCT Medium, Miles Scientific), cryostat-sectioned, and mounted onto microscope slides (SuperFrost Plus, Fisher) as described previously (Kress et al., 1990). The embryo sections were stained for β-gal, counterstained with neutral red and mounted. After staining for β-gal, some slides were processed to detect the presence of intracellular alkaline phosphatase activity (Zambrowicz et al., 1994). The appropriate reagents were supplied by Sigma, and the sections counterstained with Mayer's hematoxylin.

Immunofluorescence and immunohistochemistry

The primary antibodies used were the rat anti-Kit (ACK2) monoclonal antibody (Ogawa et al., 1991), a rabbit anti-β-gal (Cappel), and the rabbit αPEP8 (TRP-2) polyclonal antibody (Tsukamoto et al., 1992). The secondary antibodies used were a goat anti-rat IgG-FITC, anti-rabbit IgG-biotin or -TRITC conjugates (Sigma). Kit and TRP-2 were detected as previously described (Ogawa et al., 1991; Pavan and Tilghman, 1994). For the immunodetection of the β-gal, the primary antibody was diluted at 1/1000 in PBS, and the slides were then processed as described for TRP-2.

RESULTS

Generation of a new null mutation at the *W/Kit* locus

To disrupt the c-*kit* gene, we used a replacement-type targeting vector, which contained successively 1.2 kb of 5′ homology region extending from the upstream region of c-*kit* to the first exon, a nls*lacZ*-neo expression cassette, and 6.1 kb of 3′ homology region corresponding to the proximal part of c-*kit* first intron. Homologous recombination resulted in a deletion removing codons 7 to 22 and 200 pb of the first intron, and their replacement by the coding region of nls*lacZ* and the *neo* gene (Fig. 1). The *lacZ* sequence was inserted in frame with the first six codons of c-*kit*. The CK35 ES cell was electroporated with the targeting vector. Five independent homologous recombinant clones were identified by Southern blotting, giving a frequency of homologous recombination of 2.5% per G418-resistant colonies. Four chimaeric males, obtained from two independent clones, transmitted the disrupted allele when mated with either C57BL/6 or 129/Sv females. The new mutation at the *W/Kit* locus was called W^{lacZ}.

129/Sv W^{lacZ}/+ mice appeared healthy. They had white feet and a white tail tip. When heterozygotes were intercrossed, about 25% of progeny carried two copies of the novel 6.4 kb *Eco*RI targeted fragment (Fig. 2). These homozygous newborn mice were pale and rapidly died of a severe macrocytic and hyperchromic anemia. To ensure that the targeting event produced a truly null phenotype, W^{lacZ}/W^{lacZ} embryos were examined for both residual mRNA and protein. Neither c-*kit* mRNA nor Kit were detected (data not shown). Thus, as predicted, the introduced cassette prevents c-*kit* expression. We have therefore generated a null allele, W^{lacZ}, at the *W*/*Kit* locus.

LacZ expression in known target cells of *W* mutations

LacZ expression pattern was studied in +/+, W^{lacZ}/+ and

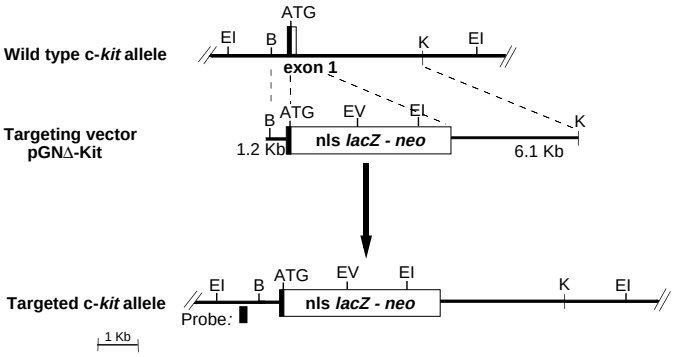

Fig. 1. c-*kit* targeting scheme. A partial map of a mouse genomic DNA fragment containing c-*kit* exon 1 is shown. Restriction enzymes: B, *Bam*HI; EI, *Eco*RI; EV, *Eco*RV; K, *Kpn*I. The targeting vector, pGNΔKit, includes the nls*lacZ*-neo cassette flanked by a 1.2 kb fragment located 5′ of exon 1 and a 6.1 kb fragment of 3′ homology. The structure of the targeted allele is indicated, with the c-*kit* exon 1 replaced by the cassette nls*lacZ*-neo. The probe used for Southern blots is shown below the map of the targeted allele.

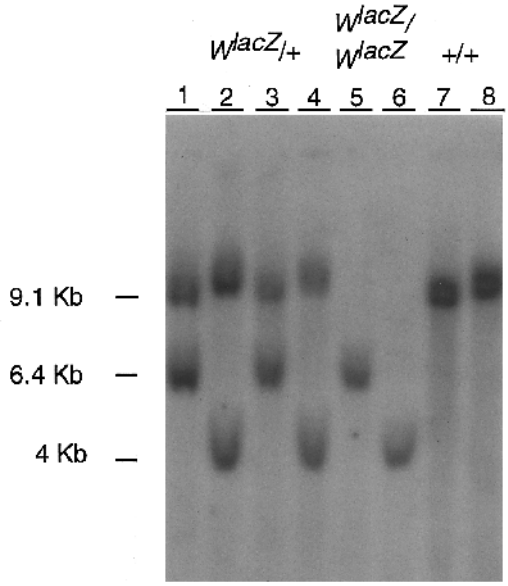

Fig. 2. Southern blot analysis of the ES cell line DNA targeted with the pGNΔKit vector (lanes 1 and 2), and of mouse tail DNA from an heterozygote intercross litter (lanes 3 to 8). Genomic DNA was prepared from W^{lacZ}/W^{lacZ} (lanes 5 and 6), $W^{lacZ}/+$ (lanes 3 and 4) and wild type +/+ (lanes 7 and 8) newborn mice. DNA samples were digested with *Eco*RI (lanes 1, 3, 5, 7) or with *Eco*RI and *Eco*RV (lanes 2, 4, 6, 8). A 300 pb *Alu*I-*Alu*I probe was used to distinguish wild type and mutant alleles. The 6.4 kb *Eco*RI and 4 kb *Eco*RI-*Eco*RV bands represent the targeted allele compared with the 9.1 kb band of the endogenous c-*kit* allele, obtained following either *Eco*RI or *Eco*RI-*Eco*RV digestion.

W^{lacZ}/W^{lacZ} embryos. No β-gal-positive cells were seen in any of the analyzed wild-type embryos. Since melanoblasts, PGC, hematopoietic progenitors and ICC express c-*kit* and are affected by mutations at the *W*/*Kit* locus (Orr-Urtreger et al., 1990; Motro et al., 1991; Keshet et al., 1991; Huizinga et al., 1995), we first studied the effects of the W^{lacZ} mutation within these four cellular lineages.

Neural-crest-derived melanocytes

To test that *lacZ* expression in the skin was identifying melanocytes, we first examined the histochemical staining for β-gal activity in neonatal skin of $W^{lacZ}/+$ and W^{lacZ}/W^{lacZ} newborn mice. In the heterozygous mice, melanocytes were found in hair follicles, in the dermis and in the basal layer of the epithelium; they displayed high β-gal activity (Fig. 3A). The cells were also stained with both anti-Kit and anti-β-gal antibodies. Their identity as melanocytes was confirmed by TRP-2 expression (data not shown). TRP-2, a melanogenic enzyme with DOPAchrome tautomerase activity, is a melanoblast marker (Tsukamoto et al., 1992; Pavan and Tilghman, 1994). Furthermore, melanocytes were absent from the skin of W^{lacZ}/W^{lacZ} newborn mice (Fig. 3B).

We therefore looked for *lacZ* expression in melanoblasts of $W^{lacZ}/+$ and W^{lacZ}/W^{lacZ} embryos. During embryogenesis, melanoblasts were identified on the basis of their location, corresponding closely to the pattern of TRP-2 distribution recently described (Cable et al., 1995); moreover, melanoblasts were stained with the anti-Kit and anti-β-gal antibodies and showed high β-gal activity. In $W^{lacZ}/+$ embryos, β-gal-positive cells were observed, from E9.5 to E13.5, on the dorsal part of the neural tube along the rostrocaudal axis. Stained melanoblasts appeared at E10.5, simultaneously on both sides of the embryo, first in the head, then in the trunk and the tail. From this stage, melanoblasts were observed migrating as a diffuse stream from the dorsal part of the neural tube to the distal parts of the body (Fig. 3C at E11.5), and proliferating in the mesenchyme beneath the surface ectoderm (Fig. 3D in the pinna at E12.5). This observation suggested the existence of a single and continuous wave of melanoblasts migration. At E15.5, melanoblasts reached the ventral parts of the body. Due to the absence of one functional allele, $W^{lacZ}/+$ melanoblasts failed to colonize the distal parts of the limb buds and of the tail tip, resulting in the dominant phenotype observed in $W^{lacZ}/+$ adults. From E16 onwards, melanoblasts began to colonize the hair follicles, and as a consequence the surface of embryos became unstained.

In W^{lacZ}/W^{lacZ} embryos, from E9.5 to E13.5, β-gal-positive cells were still found on the dorsal part of the neural tube (Fig. 3E). The consequence of the absence of Kit on melanoblasts was observed as early as E10.5, i.e. when melanoblasts begin to migrate in the mesenchyme. At E10.5, rare clusters of three to five melanoblasts were detected in the head near the pineal bud and the nasal pit. Few isolated melanoblasts were found closely associated with endothelial cells. From E11 onwards, melanoblasts were absent from the surface ectoderm of W^{lacZ}/W^{lacZ} embryos (see in Fig. 3F), and no β-gal-positive cells were ever observed in the trunk section of W^{lacZ}/W^{lacZ} embryos.

These data specify that both the migration and survival of melanoblasts are severely impaired from E15.5 in embryos lacking one functional allele of c-*kit*, and from E10.5 onwards in the null mutant embryos. Furthermore, we suggest that melanoblast migration begins at E10.5 and consists of a single and continuous wave, impaired by Kit absence.

Germ cell lineage

As Kit is expressed in germ cells of neonatal ovaries, we first examined the *lacZ* expression patterns in ovaries of $W^{lacZ}/+$

and W^{lacZ}/W^{lacZ} newborn mice. At birth, a high β-gal activity was observed in most oocytes of ovaries of heterozygous newborn mice (Fig. 4A). By contrast, no β-gal-positive cells were found in ovaries of W^{lacZ}/W^{lacZ} newborn mice (Fig. 4B), indicating that the migration, proliferation and/or survival of germ cells is severely impaired in W^{lacZ}/W^{lacZ} embryos.

We looked for β-gal activity in PGC of $W^{lacZ}/+$ and W^{lacZ}/W^{lacZ} embryos. During embryogenesis, PGC were identified on the basis of their location and intracellular alkaline phosphatase enzyme activity (Manova et al., 1990; Buehr et al., 1993; Mintz and Russell, 1957). These cells were also detected with the anti-Kit and anti-β-gal antibodies. Finally, alkaline phosphatase-positive cells showed β-gal activity. Before E9.5, no difference in the PGC distribution was observed between $W^{lacZ}/+$ and W^{lacZ}/W^{lacZ} embryos. At E9.5, PGC migrated differently, depending on the presence or absence of Kit. β-gal-positive PGC were mostly seen dispersed in the wall of the gut in $W^{lacZ}/+$ embryos. In contrast, β-gal-positive PGC were focused in the ventral half of the gut in W^{lacZ}/W^{lacZ} embryos (Fig. 4C), and were sometimes grouped in clumps located at ectopic sites such as inside the vitelline artery (data not shown). These clumps were never found in $W^{lacZ}/+$ embryos. From E10.5 onwards, a marked diminution of β-gal activity of PGC was observed in $W^{lacZ}/+$ and W^{lacZ}/W^{lacZ} embryos. Hence, the migration of PGC towards the gonadal ridges was difficult to follow on histological sections. From E11.5 to E12.5 the PGC reach the gonadal ridges. At E12.5 a very faint labelling, following histochemical staining for β-gal activity or immunostaining with anti-β-gal antibodies, was detected in the gonadal ridges of $W^{lacZ}/+$ embryos. This faint expression was not found in homozygous mutant embryos.

Differences in the expression level of the *lacZ* gene product and the endogenous c-*kit* gene were detected in PGC from E10.5 to E13.5. β-gal activity was weak in PGC, in contrast with the strong expression of the endogenous c-*kit* gene, as determined after immunofluorescence staining with the anti-Kit antibody. The deviation in the level of expression of β-gal from that of the endogenous Kit protein might derive from the deletion of a regulatory region from the targeting construct.

Altogether, our results confirm that in the absence of Kit, migration and survival of PGC are impaired in W^{lacZ}/W^{lacZ} embryos from E9.5 onwards.

Hematopoiesis

Mammalian hematopoiesis was believed to take place in two embryonic sites: first in the yolk sac and later in the fetal liver. However, additional hematopoietic activity was recently located in the intraembryonic mesodermal region, including the dorsal aorta and uro-genital ridges, the so-called AGM (for aorta, gonad and mesonephros), in the E8 to E11.5 mouse embryos (Godin et al., 1995; Dzierzak and Medvinsky, 1995). As Kit is expressed on fetal and adult murine hematopoietic cells (Ogawa et al., 1993), we looked for *lacZ* expression in $W^{lacZ}/+$ and W^{lacZ}/W^{lacZ} embryos in the three sites where an hematopoietic stem cell activity had been found. Immunoreactions using either anti-Kit or anti-β-gal antibodies stained the same cells (data not shown).

From E7.5 to E9.5, β-gal-positive cells were detected in the blood islands of the yolk sac of $W^{lacZ}/+$ and W^{lacZ}/W^{lacZ} embryos (Fig. 5A). From E9.5 to E13.5, we observed β-gal-positive cells in the AGM of both heterozygous and homozygous mutant embryos. The number of β-gal-positive cells in

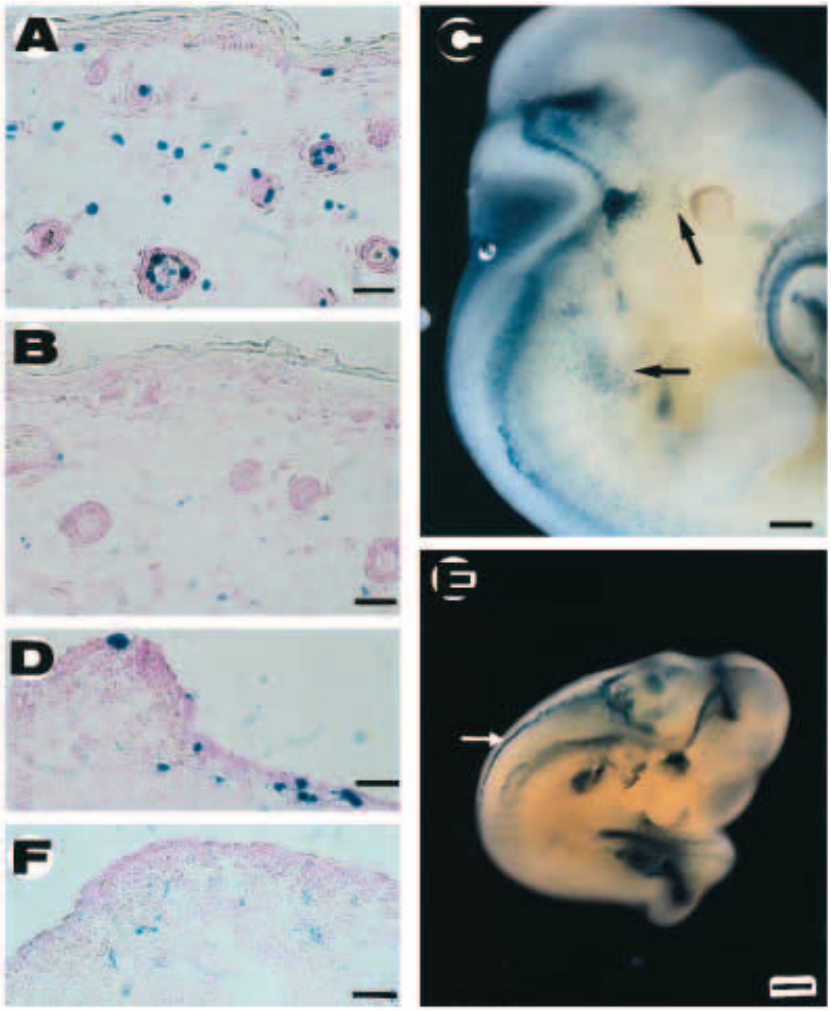

Fig. 3. *LacZ* expression in neural-crest-derived melanocytes. (A) $W^{lacZ}/+$, newborn mice. Head section: β-gal activity in hair follicles is restricted to melanocytes with a pigmented cytoplasm. In the dermis, β-gal-positive cells probably include melanoblasts and mast cells, the latter first appearing at this site between E15 and E16. (B) W^{lacZ}/W^{lacZ}, newborn mice. A similar section showing the absence of melanocytes and mast cells within the skin. (C) $W^{lacZ}/+$ embryo, E11.5. In situ detection of β-gal activity: the arrows indicate melanoblasts, visualized as blue cells distributed in the mesenchyme and surface ectoderm. (D) $W^{lacZ}/+$ embryo, E12.5. Melanoblasts (blue) are present in the surface ectoderm and underlying mesenchyme of the pinna. (E) W^{lacZ}/W^{lacZ} embryo, E9.5. Whole-mount staining showing the β-gal-positive cells along the dorsal midline of the neural tube (white arrow). (F) W^{lacZ}/W^{lacZ} embryo, E12.5. Melanoblasts are absent from the section of the pinna. Scale bars: A, B, D and F, 30 μm; C, 0.35 mm; E, 0.25 mm.

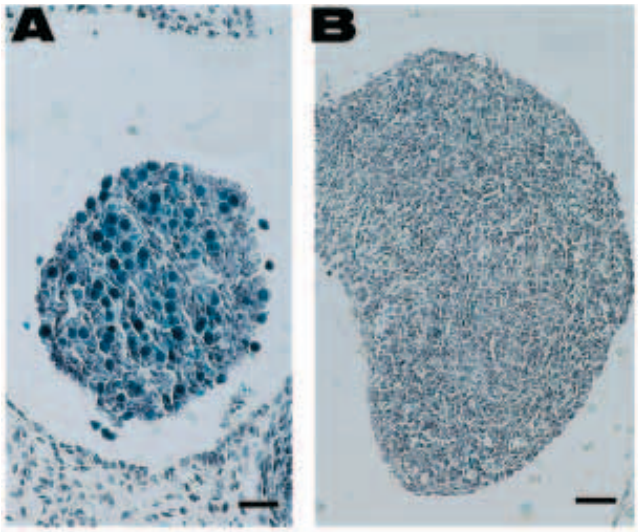

Fig. 4. *LacZ* expression in the PGC. (A) $W^{lacZ}/+$, newborn mice. β-gal-positive oocytes are present in ovary. (B) W^{lacZ}/W^{lacZ}, newborn mice. β-gal-positive cells are absent from ovary. (C) W^{lacZ}/W^{lacZ} embryo, E9.5. PGC, identified as alkaline phosphatase-positive cells, are visualized by a red cytoplasmic staining (arrows). β-gal-positive PGC are found in the ventral part of the hindgut (hg) endoderm. Scale bars: A and B, 30 μm; C, 15 μm.

the AGM increased from E9.5 to E11.5 and dropped at E12.5. The cells were observed inside the aortic wall of the dorsal aorta and in the umbilical arteries. Cells were mostly distributed on the ventral part of the aorta (Fig. 5B). As exemplified in Fig. 5C, β-gal-positive cells seemed to cross the ventral aortic endothelium and directly enter the blood; these cells would probably seed the liver and the thymus. In the liver of $W^{lacZ}/+$ and W^{lacZ}/W^{lacZ} embryos, β-gal-positive cells were first detected at E10.5; their number increased until E11.5 (Fig. 5D), and decreased from E12 onwards in embryos of both genotypes. At E15.5, a difference was observed between the liver of the embryos depending on their genotype: the number of stained cells in the liver of W^{lacZ}/W^{lacZ} embryos was considerably lower than was found in the liver of $W^{lacZ}/+$ embryos. Finally at birth, the spleen of homozygous mutant mice lacked the β-gal-positive cells found in the spleen of heterozygotes and was threefold smaller.

Due to the *lacZ* expression in hematopoietic stem and committed cells, our study allowed the spatial and temporal vizualisation of the Kit-positive cells of the AGM, as well as the migration of these cells in the blood. The cells were detected in W^{lacZ}/W^{lacZ} embryos, indicating that c-*kit* is not required for the hematopoietic cells of the AGM.

Interstitial cells of Cajal

The interstitial cells of Cajal (ICC) are believed to be responsible for the electrical activity of the intestine muscle layers (Thuneberg, 1982; Langton et al., 1989). Recently, it was reported that ICC express c-*kit*, and are dependent on its expression. Indeed, adult W/W^V mice lack the network of ICC, and their ileum fails to display any slow-wave-type action

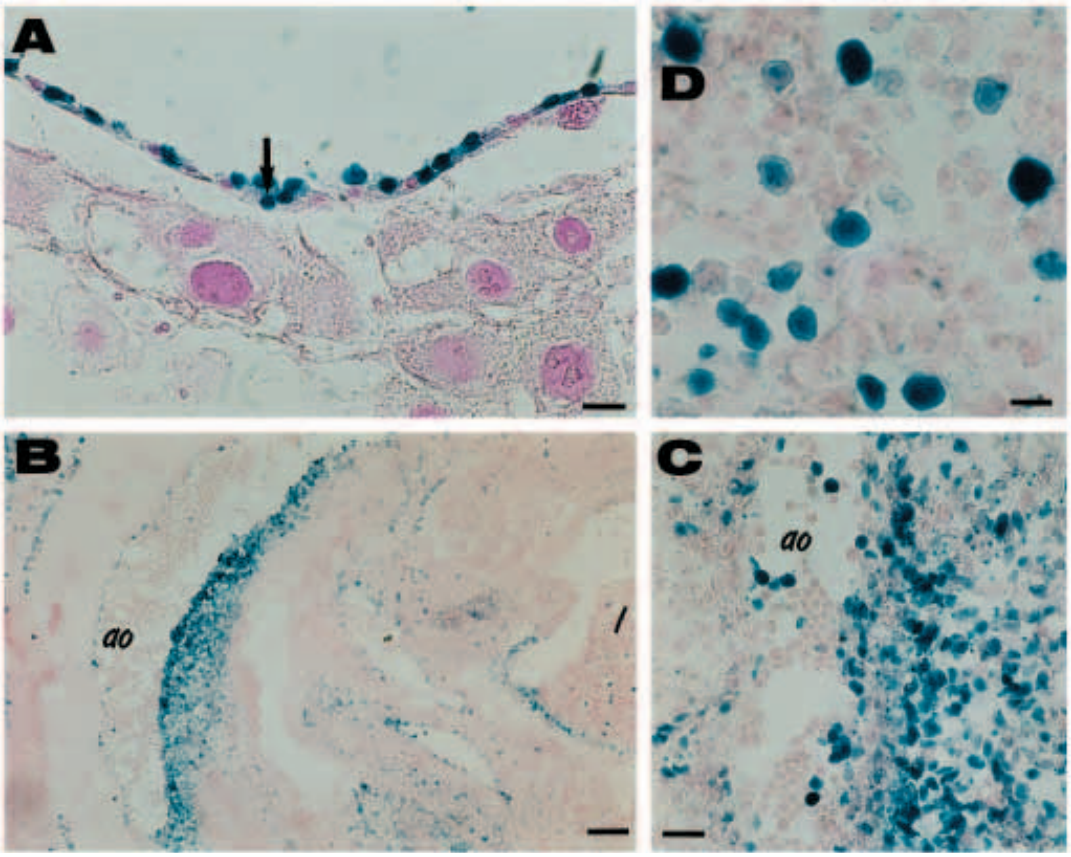

Fig. 5. *LacZ* expression observed in the embryonic hematopoietic sites. (A) W^{lacZ}/W^{lacZ} embryo, E8.5. β-gal activity is present in the yolk sac. The expression was observed in the hematopoietic progenitors of the blood islands (arrow). (B) Sagittal section of a W^{lacZ}/W^{lacZ} embryo, E11.5. β-gal activity is observed in the AGM, and the activity is essentially concentrated in the ventral part of the aorta. On the sections of homozygous mutant embryos, no PGC, as detected by alkaline phosphatase activity, is observed at this site. (C) The same embryo, at a higher magnification. (D) $W^{lacZ}/+$ embryo, E11.5. β-gal activity in the liver. ao, aorta; l, liver. Scale bars: A, 25 μm; B, 120 μm; C, 30 μm; D, 10 μm.

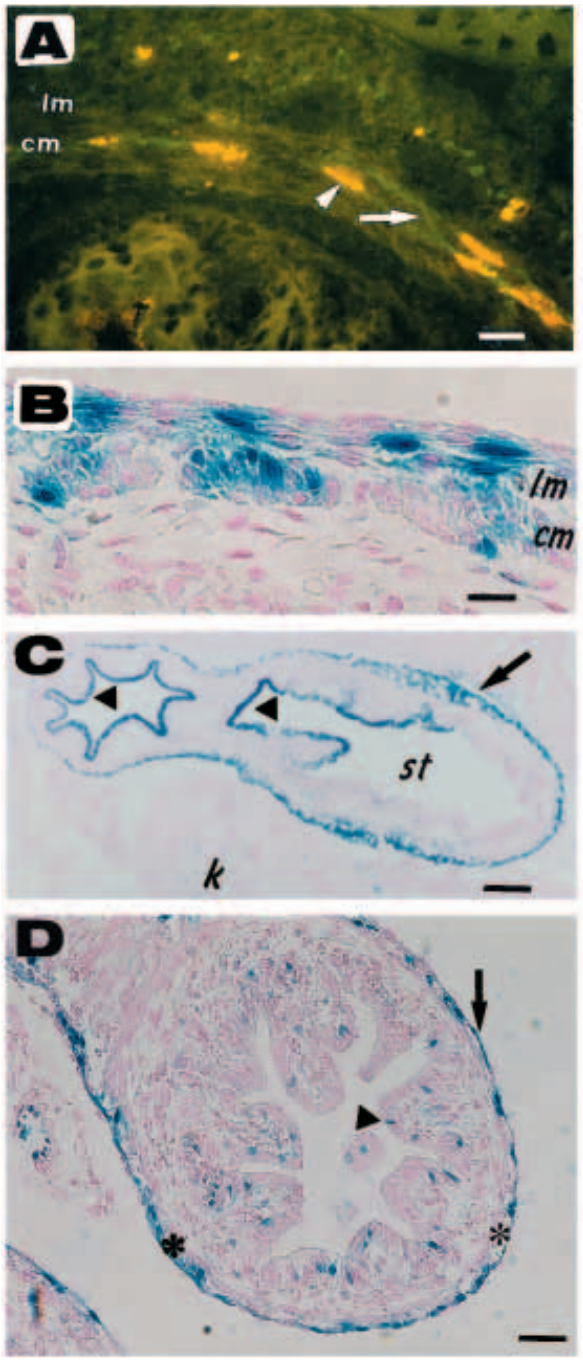

Fig. 6. *LacZ* expression in ICC. (A) W^{lacZ}/+, newborn mice, transverse section of the small intestine. Kit expression in ICC is visualized by immunofluorescence as a green membranous labelling (arrow), whereas the β-gal protein is detected as an orange nuclear staining (arrowhead). ICC are found in both external longitudinal and inner circular layers of the smooth muscle cells. (B) W^{lacZ}/+, newborn mice, longitudinal section. ICC (blue) in the stomach are found in both external longitudinal and inner circular layers of the smooth muscle cells. (C) Sagittal section, W^{lacZ}/+ embryo, E15.5. β-gal activity (blue) is detected in the smooth muscle layers of the stomach (arrow). High activity is also found in epithelial cells of the stomach pyloric part (arrowhead). The epithelial cells of the non-pyloric part of the stomach show no *lacZ* expression. (D) W^{lacZ}/W^{lacZ} embryo, E16.5, transverse section of the colon. The arrow shows the ICC surrounding myenteric plexus. Another site of *lacZ* expression was found in epithelial intestinal cells (arrowhead). cm, circular muscle layers; k, kidney; lm, longitudinal muscle layers; st, stomach; *, myenteric plexus. Scale bars: A, 50 μm; B,15 μm; C,190 μm; D, 40 μm.

potentials (Huizinga et al., 1995). We analyzed the Kit expression in the digestive tract of W^{lacZ}/+ newborn mice. Kit-positive cells were found in the outer longitudinal and in the inner circular smooth muscle layers of the small intestine. The cells were elongated, and parallel to the axis of the intestine. Few of these surrounded the myenteric ganglia. Both anatomical criteria and Kit expression allowed us to identify these cells as ICC (Faussone-Pellegrini, 1985; Huizinga et al., 1995). A high β-gal immunoreactivity was also detected in the ovoid nucleus of ICC of the small intestine (Fig. 6A). Kit- and β-gal-positive ICC were found from the oeseophagus to the anus. Many were found in the gastroduodenal junction, in each muscle layer of the stomach (Fig. 6B), in the colon and caecum. By contrast, ICC were less numerous in the pyloric part of the stomach and scattered in the ileum. This difference in ICC number, depending on the digestive tract part, was observed as early as *lacZ* is expressed. Indeed, during embryogenesis, *lacZ* expression in ICC was detected from E12.5 and E13.5 onwards in all the digestive tract sections of W^{lacZ}/+ embryos. Fig. 6C shows ICC in the stomach at E15.5. β-gal activity in ICC persisted until birth.

In W^{lacZ}/W^{lacZ} embryos, the ICC *lacZ* expression pattern was identical to the pattern observed in W^{lacZ}/+ embryos, as exemplified on Fig. 6D in the colon at E16.5. Therefore, Kit function is not required for ICC migration, proliferation and/or survival during embryogenesis.

Taken together, these results indicated that during embryogenesis, (1) ICC express Kit and (2) ICC do not require c-*kit* for their migration, proliferation and/or survival.

LacZ expression in lineages not known to be affected by *W* mutations

The fidelity of the *lacZ* gene introduced into the c-*kit* gene was established in the W^{lacZ}/+ embryos by the identity between the patterns obtained after histochemical staining for β-gal activity and immunostaining with the anti-Kit antibody (data not shown). Thus *lacZ* expression reflected normal expression of the c-*kit* gene.

Many cells with β-gal activity were found in W^{lacZ}/W^{lacZ} as well as in W^{lacZ}/+ embryos, indicating that these cells do not require c-*kit* function during embryogenesis.

Early development

Faint β-gal activity first appeared at the late 2-cell stage, and persisted in some blastomeres at later stages. In the blastocyst, isolated β-gal-positive cells were observed in the trophectoderm and the inner cell mass (not shown). We searched for *lacZ* expression in the targeted ES cells. About 30% of the c-*kit* mutated ES cells showed a high β-gal activity.

Skeleton

Chondrocytes expressing the *lacZ* gene were detected for the first time at E13.5. More β-gal-positive chondrocytes were found from E15.5 onwards (see at E16.5 on Fig. 7A). In newborn mice, β-gal activity was clearly observed in mature

and proliferating chondrocytes of few ossification centers. This activity was not detected in all the cells, and varied from faint to strong.

Tooth development

β-gal-positive cells were found in the primordia of the teeth bud from E16.5 to birth (not shown).

Brain and neural tube

Analysis of the developing brain showed an extensive staining, particularly in the cerebellum, hippocampus, choroid plexus and telencephalon. In the neural tube, β-gal activity was found in the dorsolateral marginal zone, and the level of *lacZ* expression was higher in dorsal than in ventral parts.

β-gal-positive cells were also found in several cranial ganglia. The trigeminal (V), facial (VII), cochlear (VIII), glossopharyngeal (IX) and vagal (X) ganglia contained many β-gal-positive cells from E9.5 to birth. β-gal-positive cells were observed at E9.5 in neural-crest-derived spinal ganglia, whose cells give rise to the sensory cells of dorsal root ganglia (DRG). Indeed, some β-gal-positive cells were found in DRG, from E11.5 to newborn animals, together with other DRG cells that were not stained (see at E15.5, on Fig. 7B).

Sensory organs

In the eye, β-gal-positive cells were found in two distinct locations from E14.5 onwards: in the lens and in the neural layer of retina, in both the inner and outer nuclear layers (see Fig. 7C at E16.5). In the ear, β-gal-positive cells were found in the first branchial membrane at E9.5. This labelling persisted at birth in the epithelium of the future tympanic membrane and in the pharyngo-tympanic (Eustachian) tube (not shown).

The respiratory system

β-gal activity was found in the endodermal lining of the respiratory tube. The epithelial cells of the olfactory epithelium were detected as expressing the *lacZ* gene from E10.5 onwards. After E15.5, a high expression level of the *lacZ* gene appeared in several other locations: in all the cells of the nasopharynx (Fig. 7D), in a few cells of the trachea and bronchi, and in most cells of the lungs. The *lacZ* expression pattern persisted until birth.

The digestive system

From E7.5 onwards, the foregut cells expressed the *lacZ* gene. At E10.5 β-gal activity appeared in the caudal half of the stomach epithelium and in the hind- and mid-gut epithelium. From E14.5 onwards, β-gal-positive cells were found in all sections of the gut epithelium. In newborn mice, β-gal activity was found in epithelial cells of each portion of the digestive tract. In the anterior part of the digestive system, β-gal-positive epithelial cells were seen in the bucco- and oro-pharynx, the larynx, the oral epithelium, the tongue and the oesophagus (Fig. 7E). In the stomach, most β-gal-positive cells were found in the pyloric half of the epithelium (see above, Fig. 6B). Many β-gal-positive cells were found in the intestine, but only scattered cells expressed β-gal activity in the rectum. Intestinal epithelial cells are a mixed population of enterocytes, Paneth cells, Goblet cells and neuroendocrine cells. Each of these cell types expressed the *lacZ* gene, although not all cells were stained.

β-gal activity was also observed in the endodermal lining of

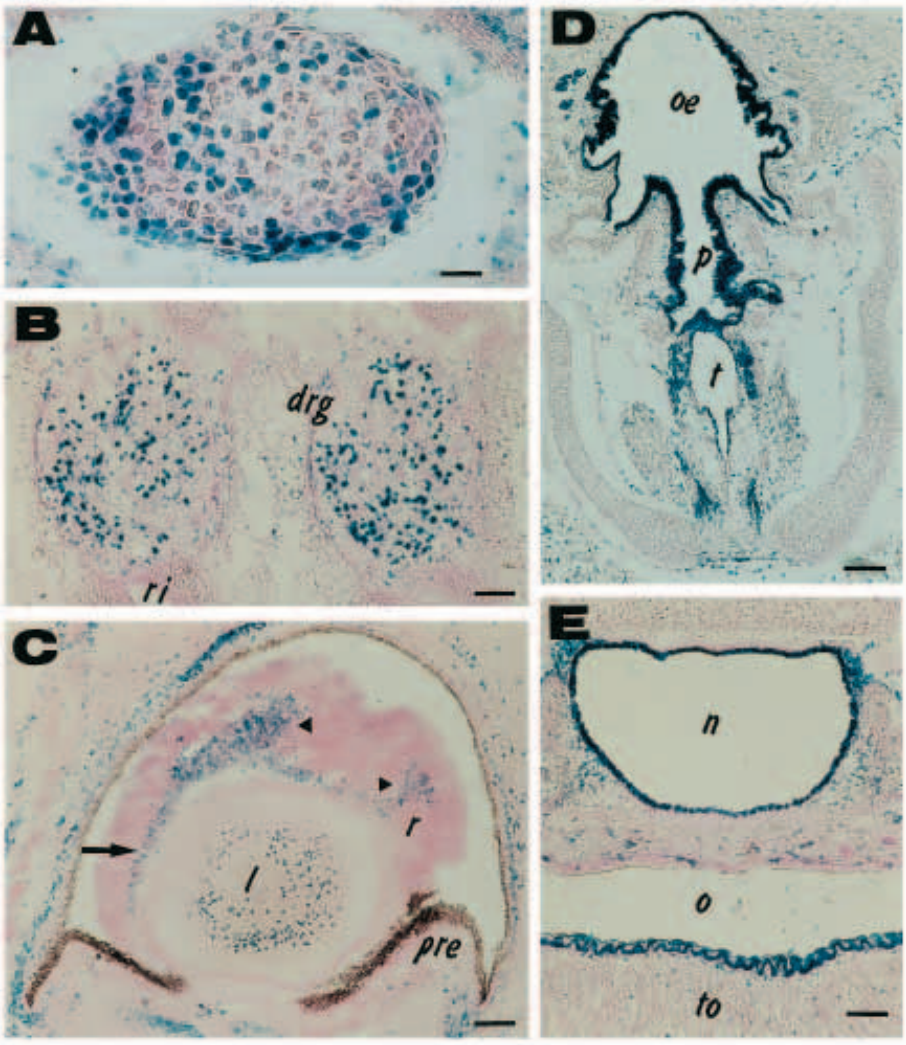

Fig. 7. Analysis of *lacZ* expression patterns in various sites of W^{lacZ}/W^{lacZ} embryos. (A) E16.5. β-gal activity (blue) in chondrocytes of a head bone. (B) E15.5. β-gal activity in dorsal root ganglia in the thoracic region. (C) E16.5. β-gal activity in the eye is detected in both the inner (arrow) and outer (arrowheads) nuclear layers of the retina. (D) E15.5. β-gal activity is seen in the epithelial cells of the oesophagus, the nasopharynx and in a few epithelial cells of the trachea. (E) Newborn mice. β-gal activity is found in all the cells constituting the epithelium of the oropharynx and on the superficial lining of the tongue. drg, dorsal root gandlia; l, lens; n, nasopharynx; oe, oesophagus; o, oropharynx; p, pharynx; pre, pigmented retina epithelium; r, retina; ri, rib; t, trachea; to, tongue. Scale bars: A, 30 μm; B, 75 μm; C, 120 μm; D, 235 μm; E, 120 μm.

digestive tract-derived glands. In digestive salivary glands, such as the submandibular gland, a few collector tube cells and glandular cells showed β-gal activity from E15.5 onwards (see at E 16.5 on Fig. 8A). The β-gal activity persisted in newborn mice. In the liver, few endodermal β-gal-positive cells were detected in newborn mice. In the biliary ducts and in the gall bladder of newborn mice, few epithelial cells were β-gal-positive. In the pancreas, at E12.5 few epithelial collector tube cells were β-gal-positive while most pancreatic cells were unstained. In newborn mice, this β-gal activity was restricted to some collector tube cells and to most cells of the Langherans islets (Fig. 8B).

Endocrine organs

β-gal-positive cells were found in several endocrine tissues. In the thyroid gland, cells with β-gal activity were first detected at E14.5. This activity persisted through to birth and was limited to cells scattered within the thyroid gland, in close association with the epithelial cells (Fig. 8C). The description closely corresponds to that of calcitonin-producing cells. In the pituitary gland primordium, scattered β-gal-positive cells were found from E15.5 onwards. At E16.5 many cells of the pars intermedia were β-gal-positive. The β-gal activity was still observed in newborn mice, restricted to most cells of the pars intermedia (Fig. 8D). The pineal gland was found to contain β-gal-positive cells at E11.5 after its evagination from the roof of the diencephalon; this β-gal activity persisted throughout embryogenesis (see at E13.5 on Fig. 8E). The Kit expression in the pineal gland was assessed by immunofluorescence at this stage (Fig. 8F). β-gal activity was found in most cells of the gland in the newborn mice. From E14.5 onwards, β-gal-positive cells were found in the adrenal gland; at birth, β-gal activity was still found in a few adrenal medulla cells.

The circulatory system

At E7.5, the mesenchymal aggregates forming the blood islands of the yolk sac were stained. The *lacZ* expression was not restricted to the hematopoietic progenitors, but was also found in vitelline veins. At E9.5, the *lacZ* expression was observed in the blood islands of the yolk sac vasculature (Fig. 9A), in the endocardium, in the endothelium of the dorsal aorta and in cells lining the intersomitic vessels (Fig. 9B). β-gal activity was detected in the endothelium of vessels from E9.5 onwards (for example, see at E13.5 in Fig. 9C). The *lacZ* expression was detected as early as E11 in the endothelial cells of the lung primordium, and persisted in newborn mice. At birth, all the cells lining vascular lumen were stained. The β-gal activity was higher in the endocardium, the arterial and capillary endothelium than in the veins, veinules and lymphatic endothelium.

The genitoexcretory system

β-gal-positive-cells were found in the urogenital system. No β-gal-positive cells were detected in the pronephros. At E11.5, β-gal activity was detected in the mesonephric tubules. From E13 onwards, β-gal-positive cells were found in the mesonephric duct (Wolffian duct) of male embryos and, in newborn males, β-gal activity was observed in cells of the ductus deferens and of the epididymis. From E14.5 onwards, β-gal-positive cells were found in the paramesonephric duct (Müllerian duct), and *lacZ* expression persisted at birth in the oviduct and in few uterine horn cells. From E12.5 onwards, β-

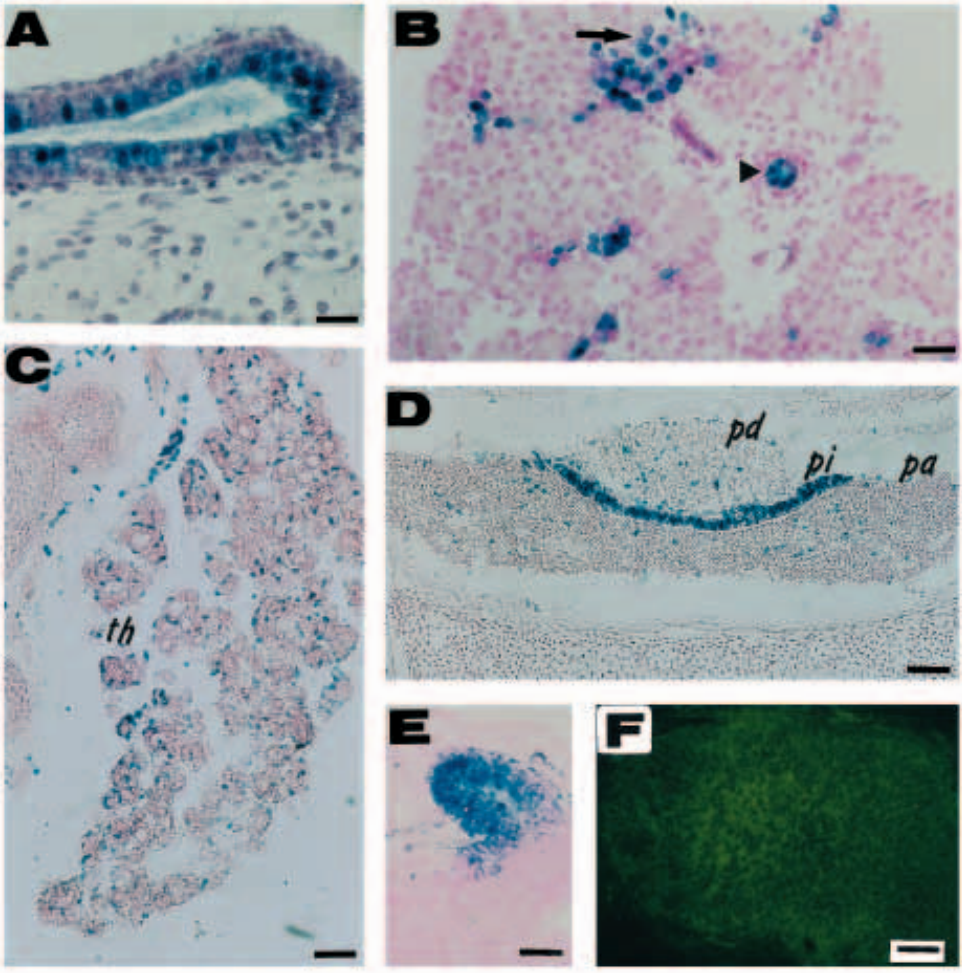

Fig. 8. *LacZ* expression in endocrine organs. (A) W^{lacZ}/W^{lacZ} embryos, E16.5. β-gal activity (blue) is found in collector tubes of the mandibular salivary glands. (B) W^{lacZ}/W^{lacZ} newborn mice, pancreas. β-gal activity is detected in many collector tube cells (arrowhead), as well as in Langherans islets (arrow). (C) W^{lacZ}/W^{lacZ} newborn mice. β-gal activity in the thyroid gland. (D) W^{lacZ}/W^{lacZ} newborn mice. β-gal activity in the pituitary gland is observed in most cells of the pars intermedia, as well as in a few cells of the pars distalis and the pars anterior. (E)W^{lacZ}/W^{lacZ} embryos, E13.5. β-gal activity in the pineal gland. (F) +/+ embryos, E 13.5. Kit expression (green) in the pineal gland, detected by immunofluorescence. pa, pars anterior; pd, pars distalis; pi, pars intermedia; th, thyroid. Scale bars: A and B, 30 μm; C and E, 60 μm; D, 100 μm; F, 50 μm.

gal-positive cells were observed in the metanephros, and in the ureters. In newborn mice, β-gal-positive cells were also found among the epithelial cells of collector and distal tubes. The bladder and ureter epithelial cells exhibited β-gal activity in newborn mice (not shown).

DISCUSSION

In situ hybridization of ^{35}S-labelled RNA probes to embryo sections was previously used to investigate the tissue distribution of c-*kit* transcripts (Orr-Urtreger et al., 1990; Keshet et al., 1991; Motro et al., 1991). However, conventional in situ hybridization has severe limitations, including the fact that a clear identification of the individual cell expressing the gene is not always possible. Immunohistochemistry has been successfully used to detect Kit expression (Ogawa et al, 1991; Cable et al., 1995; Huizinga et al., 1995). However, Kit expression cannot be followed in embryos homozygous for a null mutation in the c-*kit* gene.

We have taken advantage of the convenient nls*lacZ* reporter gene since it provides an easily detectable, highly sensitive and resolutive marker. Furthermore, its product is non-deleterious for the embryo. The replacement of the first exon of c-*kit* by the *lacZ* gene enables β-gal expression to faithfully recapitulate the endogenous c-*kit* expression. Through a cell by cell observation, the marker enabled us to follow the fate of cells that express and require c-*kit* during embryogenesis. Indeed, the disappearance of *lacZ*-expressing cells in embryos homozygous for the null mutation allowed the determination of where and when the cells of the affected lineage fail to survive in the absence of c-*kit*. Furthermore, novel sites of c-*kit* expression were identified during embryogenesis; these include ICC, but also endothelial, epithelial and endocrine cells.

ICC are Kit-independent during embryogenesis

ICC generate electrical rhythmicity and mediate neural inputs in the gastrointestinal tract. In vitro, freshly dispersed and cultured ICC are excitable and spontaneously rhythmic. ICC are thought to be responsible for the autonomic intestinal motility, characterized by a continuous slow-wave activity (Langton et al., 1989). ICC were identified in young and adult mice, but not in embryos (Faussone-Pellegrini, 1984, 1985). Recently, Kit was found to be expressed in ICC in newborn mice and in adults (Huizinga et al., 1995). Our analysis reveals that c-*kit* is expressed in ICC from E13.5 onwards. Thus, the W^{lacZ} allele provides a useful marker to study the ICC lineage. In the stomach, ICC were found to form part of the inner muscle cell bundles, in accordance with experiments showing a mesodermal origin of ICC (Lecoin et al., 1996).

Two observations indicate that, in postnatal life, ICC survival requires c-*kit* expression. First, anti-Kit antibody injections between 0 to 4 days post partum abolish highly autonomic phasic contractions. Second, ilea of W/W^V adults lack the network of ICC (Huizinga et al., 1995). *W* and W^V mutations have been analyzed at the molecular level. The *W* mutation is responsible for the synthesis of a non-functional protein, which is not expressed at the cell membrane, while W^V is associated with a reduced kinase activity of the receptor (Nocka et al., 1990). Hence, in W/W^V double heterozygotes only the W^V mutant Kit is found on the cell surface. By contrast, W^{lacZ}/W^{lacZ} embryos completely lack Kit protein. Thus the effects of *W* mutations on ICC is expected to be increased in W^{lacZ}/W^{lacZ} mice compared to W/W^V animals. Interestingly, the comparison of digestive tract sections of $W^{lacZ}/+$ and W^{lacZ}/W^{lacZ} mutants revealed that ICC were present in homozygous newborn mice, implying that in the absence of Kit, ICC migration, proliferation and/or survival are not impaired until birth.

In support of this conclusion, transmission electron microscopic studies have revealed that ICC differentiate at birth and are fully developed in 30-day-old animals (Faussone-Pellegrini, 1984, 1985). Therefore, c-*kit* is crucial for the ICC survival and/or differentiation in postnatal life. Nevertheless, it is worth noting that out of six *W/W* adult mice cured of anemia following an injection of hematopoietic stem cells during embryogenesis, only one suffered intussusception causing blockage in the telescoped intestinal region (Fleishmann and Mintz, 1979). This result may suggest that another receptor is able to promote ICC survival in *W/W* mice and/or that the functional necessity of ICC for the intestinal motility has been overestimated.

Endothelial cells express c-*kit*

In birds, the hemangioblast lineage (hematopoietic and endo-

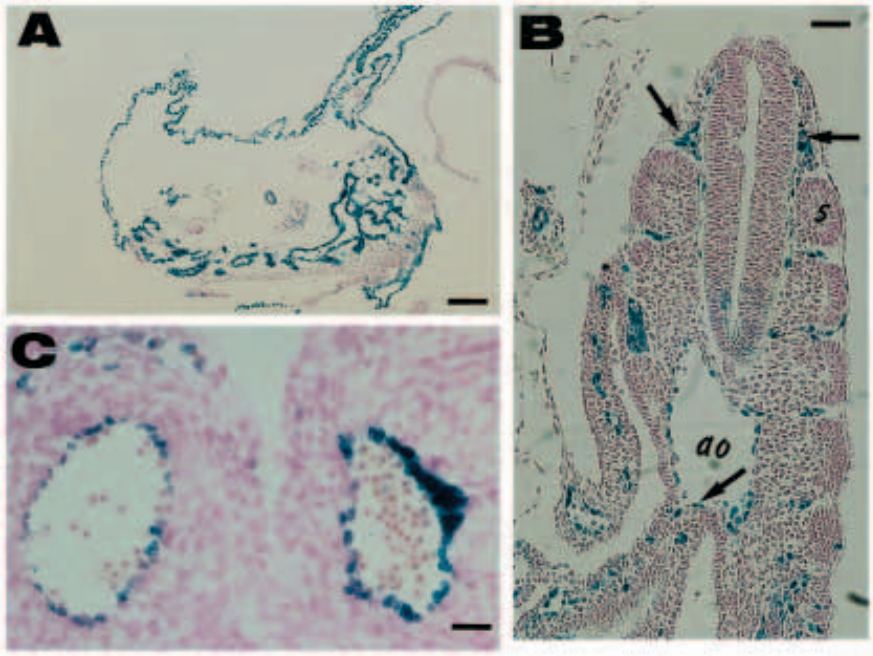

Fig. 9. *LacZ* expression in endothelial cells of W^{lacZ}/W^{lacZ} embryos. (A) E9.5. β-gal activity (blue) is observed in the yolk sac vasculature. (B) E9.5. *lacZ* expression is found in endothelial cells of the intersomitic arteries (arrows), as well as in endothelial cells of larger vessels. (C) E13.5. β-gal activity in the endothelium of vessels. s, somite; ao, aorta. Scale bars: A, 150 μm; B, 60 μm; C, 30 μm.

thelial cells) can be traced by means of Mab MB1 (Dieterlen-Lièvre and Le Douarin, 1993). In mice, it is unclear at present whether hematopoietic and endothelial cells arise from the same putative hemangioblast precursor. CD34 and GATA2 are expressed in hematopoietic stem cells and in EC (Young et al., 1995; Dorfam et al., 1992). Here, we show that c-*kit* is also expressed in both hematopoietic stem cells and EC. Therefore, we assume that the hemangioblast precursors could be considered as $CD34^+$ $GATA2^+$ Kit^+ cells.

During embryogenesis, vascularization is achieved through two different processes: vasculogenesis and angiogenesis. Vasculogenesis, i.e. the formation of blood vessels from in situ differentiating angioblasts, is considered to account for the formation of the heart, the dorsal aorta, the cardinal and vitelline vessels, as well as the extraembryonic vessels of the yolk sac. Angiogenesis, i.e. the formation of blood vessels that sprout from pre-existing vessels, is thought to be responsible for the formation of vessels such as the intersomitic arteries (Yamaguchi et al., 1993). c-*kit* expression was found in the intersomitic vessels as well as in the endothelium of the dorsal aorta, and in vessels of the yolk sac. Therefore c-*kit* is expressed during both vasculogenesis and angiogenesis.

Several RTK are important for the transduction of angiogenic stimuli. Some of them are widely expressed in several tissues and cell types, whereas others are endothelial cell-specific, including *flk-1*, *flt-1*, *tek*, *tie-1* and *tie-2*. Specific RTK play a crucial role in endothelial cell differentiation, and are necessary for the normal development of the mouse embryo vasculature (Shalaby et al., 1995; Fong et al., 1995; Dumont et al., 1994; Sato et al., 1995). In contrast, c-*kit* expression, although detected early in embryogenesis, is not required for the endothelial cell lineage, as revealed by the fact that the endothelial cell migration, proliferation and/or survival were not impaired in the absence of Kit. In human, SCF is expressed in dermic endothelial cells (Weiss et al., 1995), and both Kit and SCF are expressed by umbilical vein and adult aortic endothelial cells (Broudy et al., 1994; Buzby et al., 1994). Therefore, the Kit/SCF system may be involved in the adult in cell adhesion and migration, in vascularisation of normal or wounded tissues. Further studies should clarify the functions of the Kit/SCF system in endothelial cells and the potential involvement of the Kit/SCF system in tumor angiogenesis.

Epithelial and endocrine cells express c-*kit*

In the mouse, c-*kit* expression was found in several epithelial cells of the digestive, respiratory and genital tracts, and in several endocrine cells, including cells of the Langherans islets, adrenal medulla cells, thyroid, pineal and pituitary cells. None of these cells have been identified as c-*kit*-expressing cells before. Interestingly, the Kit-positive endocrine cells do not share the same embryological origin: neural crest for adrenal cells, ectodermic for pineal cells, and endodermic for cells of the Langherans islets; their common denominator is the c-*kit* expression. In the absence of Kit, those endocrine cells were nevertheless present in W^{lacZ}/W^{lacZ} embryos; thus they do not require Kit for their migration, proliferation and/or survival during embryogenesis. The function of Kit in endocrine cell differentiation in the adult mice remains to be studied.

It is worth noting that the receptor tyrosine kinase Ret is also expressed in acinar cells of salivary glands, in cells of the adrenal medulla and in calcitonin-producing cells of the thyroid (Tsuzuki et al., 1995). c-*ret* mutations are associated with multiple endocrine neoplasia (MEN) types 2A and 2B, with familial medullary thyroid carcinoma, and with sporadic thyroid carcinomas (Goodfellow and Wells, 1995). A c-*ret* mutation does not account for all the MEN-2A cases, nor does it explain all cases of sporadic medullary thyroid carcinoma and of MEN 2B (Goodfellow and Wells, 1995). Because c-*kit* and c-*ret* share the same transduction pathways, as shown by the fact that c-*ret* can compensate for the c-*kit* melanoblast deficiency in W/W^V mice (Iwamoto et al., 1992), and because activation of c-*kit* has been reported in association with neoplasia (Kitayama et al., 1995), we suggest that gain-of-function mutations of c-*kit* could be involved in endocrine neoplasia.

We assumed that cellular lineages other than known target cells of *W* mutations could be dependent on the Kit/SCF system. Our data show that no other cell is dependent on this system during embryogenesis. Nevertheless, it is worth noting that known target cells of *W* mutations, i.e. melanoblasts, PGC and hematopoietic progenitors, are derived from precursors that express c-*kit*, but are not dependent on its expression. Thus, several c-*kit*-positive cells, not affected by the lack of Kit in W^{lacZ}/W^{lacZ} embryos during embryogenesis, may be precursors of cells that depend on Kit for their survival, as examplified by the ICC. To test further this hypothesis, rescue of W^{lacZ}/W^{lacZ} embryos by microinjection of wild-type hematopoietic stem cells will be necessary.

We are grateful to V. J. Hearing and S.-I. Nishikawa for anti-TRP2 and anti-Kit antibodies. We would like to thank C. Babinet, M. O. Ott and F. Poirier for critically reading the manuscript. We are indebted to J. J. Fontaine, S. Hailé and M. Wassef for help during the histological analysis, and to M. L. Cadrot, S. Julé and P. Salaün for technical assistance. This work was supported by the Ministère de l'Agriculture et de la Forêt, and the Institut National de la Recherche Agronomique. The support of a fellowship from the Ligue Nationale Contre le Cancer to F. B. is gratefully acknowledged. P. D. S. is a fellow of the Association pour la Recherche contre le Cancer.

REFERENCES

Broudy, V. C., Kovach, N. L., Bennett, L. G., Lin, N., Jacobsen, F. W. and Kidd, P.G. (1994). Human umbilical vein endothelial cells display high-affinity c-*kit* receptors and produce a soluble form of the c-*kit* receptor. *Blood* **83,** 2145-2152.

Buehr, M., McLaren, A., Bartley, A. and Darling, S. (1993). Proliferation and migration of primordial germ cells in W^e/W^e mouse embryos. *Develop. Dynam.* **198,** 182-189.

Buzby, J. S., Knoppel, E. M., Cairo, M. S. (1994). Coordinate regulation of Steel Factor, its receptor (Kit), and cytoadhesion molecule (ICAM-1 and ELAM-1) mRNA expression in human vascular endothelial cells of differing origins. *Exp. Hematol.* **22**, 122-129.

Cable, J., Jackson, I. J., and Steel K. P. (1995). Mutations at the *W* locus affect survival of neural crest-derived melanocytes in the mouse. *Mech. Develop.* **50,** 139-150.

Colucci-Guyon, E., Portier, M.-M., Dunia, I., Paulin, D., Pournin, S. and Babinet, C. (1994). Mice lacking vimentin develop and reproduce without an obvious phenotype. *Cell* **79,** 679-694.

De Sepulveda, P., Peyrieras, N. and Panthier, J.-J. (1994). Instability at the *W*/c-*kit* locus in mice: analysis of melanocyte cell lines derived from reversion spots. *Oncogene* **9,** 2655-2661.

De Sepulveda, P., Salaün, P., Maas, N., Andre, C. and Panthier, J.-J. (1995). SARs do not impair position-dependent expression of a Kit/lacZ transgene. *Biochem. Biophys. Res. Commun.* **211,** 735-741.

Dieterlen-Lièvre, F., and Le Douarin, N. M. (1993). Developmental rules in

the hematopoietic and immune systems of birds: how general are they? *Dev. Biol.* **4,** 325-332.

Dorfam, D. M., Wilson, D. B., Bruns, G. A., and Orkin, S. H. (1992). Human transcription factor GATA-2. Evidence for regulation of preproendothelin-1 gene expression in endothelial cells. *J. Biol. Chem.* **267,** 1279.

Dumont, D. J., Gradwohl, G. J., Fong, G.-H., Puri, M. C., Gertsenstein, M., Auerbach, A. and Breitman, M. L. (1994). Dominant-negative and targeted null mutations in the endothelial receptor tyrosine kinase, *tek*, reveal a critical role in vasculogenesis of the embryo. *Genes Dev.* **8,** 1897-1909.

Dzierzak, E. and Medvinsky, A. (1995). Mouse embryonic hematopoiesis. *TIG* **11,** 359-366.

Faussone-Pelligrini, M. S. (1984). Morphogenesis of the special circular muscle layer and of the interstitial cells of Cajal related to the plexus muscularis profundus of mouse intestinal muscle coat. An E.M. study. *Anat. Embryol.* **169,** 151-158.

Faussone-Pelligrini, M. S. (1985). Cytodifferentiation of the interstitial cells of Cajal related to the myenteric plexus of mouse intestinal muscle coat. An E.M. study from foetal to adult life. *Anat. Embryol.* **171,** 163-169.

Fleischman, R. A. and Mintz, B. (1979). Prevention of genetic anemias in mice by microinjection of normal hematopoietic stem cells into the fetal placenta. *Proc. Natl. Acad. Sci. U.S.A.***76,** 5736-5740.

Fong, G.-H., Rossant, J., Gertsenstein, M. and Breitman, M. L. (1995). Role of the Flt-1 receptor tyrosine kinase in regulating the assembly of vascular endothelium. *Nature* **376,** 66-70.

Galli, S. J., Zsebo K. M. and Geissler E. N. (1994). The kit ligand, Stem Cell Factor. *Adv. Immunol.* **55,** 1-96.

Godin, I., Dieterlen-Lièvre, F. and Cumano, A. (1995). Emergence of multipotent hemopoietic cells in the yolk sac and paraaortic splanchnopleura in mouse embryos, beginning at 8.5 days postcoitus. *Proc. Natl. Acad. Sci. U.S.A.* **92,** 773-777.

Goodfellow, P. J. and Wells, S. A. (1995). Ret gene and its implications for cancer. *J. Nat. Cancer Inst.* **87,** 1515-1523.

Huizinga, J. D., Thuneberg, L., Klüppel, M., Malysz, J., Mikkelsen, H. B., and Bernstein, A. (1995).*W*/Kit gene required for interstitial cells of Cajal and for intestinal pacemaker activity. *Nature* **373,** 347-349.

Iwamoto, T., Takahashi, M., Ohbayashi, M. and Nakashima, I. (1992). The *ret* oncogene can induce melanogenesis and melanocyte development in W^v/W^v mice. *Exp. Cell Res.* **200,** 410-415.

Keshet, E., Lyman, S. D., Williams, D. E., Anderson, D. M., Jenkins, N. A., Copeland, N. G. and Parada, L.F. (1991). Embryonic RNA expression patterns of the c-*kit* receptor and its cognate ligand suggest multiple functional roles in mouse development. *EMBO J.* **10,** 2425-2435.

Kitayama, H., Kanakura, Y., Furitsu, T., Tsujimura, T., Oritani, K., Ikeda, H., Sugahara, H., Mitsui, H., Kanayama, Y., Kitamura, Y. and Matsuzawa, Y. (1995). Constitutively activating mutations of c-*kit* receptor tyrosine kinase confer factor-independent growth and tumorigenicity of factor-dependent hematopoietic cell lines. *Blood* **85,** 790-798.

Kress, C., Vogels, R., De Graaf, W., Bonnerot, C., Meijlink, F., Nicolas, J.-F. and Deschamps, J. (1990). Hox-2.3 upstream sequences mediate lacZ expression in intermediate mesoderm derivatives of transgenic mice. *Development* **109,** 775-786.

Langton, P., Ward, S. M., Carl, A., Norell, M. A. and Sanders, K. M. (1989). Spontaneous electrical activity of interstitial cells of Cajal isolated from canine proximal colon. *Proc. Natl. Acad. Sci. USA* **86,** 7280-7284.

Lecoin, L., Gabella, G. and Le Douarin, N. (1996). Origin of the c-*kit*-positive cells in the avian bowel. *Development* **122,** 725-733.

Le Mouellic, H., Lallemand, Y. and Brûlet, P. (1990). Targeted replacement of the homeobox gene *Hox-3.1* by the *Escherichia coli lacZ* in mouse chimeric embryons. *Proc. Natl. Acad. Sci. USA* **87,** 4712-4716.

Manova, K., Nocka, K., Besmer, P. and Bachvarova, R. F. (1990). Gonadal expression of c-*kit* encoded at the *W* locus of the mouse. *Development* **110,** 1057-1069.

Matsui, Y., Zsebo, K. M. and Hogan, B. L. M. (1990). Embryonic expression of a haematopoietic growth factor encoded by the *Sl* locus and the ligand for c-*kit*. *Nature* **347,** 667-669.

Mintz, B. and Russell, E. S. (1957). Gene-induced embryological modifications of primordial germ cells in the mouse. *J. Exp. Zool.* **134,** 207-237.

Motro, B., Van der Koy, B., Rossant, J., Reith, A. and Bernstein, A. (1991). Contiguous patterns of c-*kit* and *steel* expression: analysis of mutations at the *W* and *Sl* loci. *Development* **113,** 1207-1221.

Nocka, K., Tan, J. C., Chiu, E., Chu, T. Y., Ray, P., Trakman, P. and Besmer, P. (1990). Molecular bases of dominant-negative and loss of function mutations at the murine c-*kit*/white spotting locus: W^{37}, W^V, W^{41}, and *W*. *EMBO J.* **9,** 1805-1813.

Ogawa, M., Matsuzaki, Y., Nishikawa, S., Hayashi, S.-I., Kunisada, T., Sudo, T., Kina, T., Nakauchi, H. and Nishikawa, S.-I. (1991). Expression and function of c-*kit* in hemopoietic progenitor cells. *J.Exp.Med.* **174,** 63-71.

Ogawa, M., Nishikawa, S., Yoshinaga,K., Hayashi, S.-I., Kunisada, T., Nakao, J., Kina, T., Sudo, T., Kodama, H. and Nishikawa, S.-I. (1993). Expression and function of c-*kit* in fetal hemopoietic progenitor cells: transition from the early c-kit-independent to the late c-kit-dependent wave of hemopoiesis in the murine embryo. *Development* **117,** 1089-1098.

Orr-Urtreger, A., Avivi, A., Zimmer, Y., Givol, D., Yarden, Y. and Lonai, P. (1990). Developmental expression of c-*kit*, a proto-oncogene encoded by the *W* locus. *Development* **109,** 911-923.

Pavan, W. J. and Tilghman, S. M. (1994). Piebald lethal (s^l) acts early to disrupt the development of neural crest-derived melanocytes. *Proc. Natl. Acad. Sci. USA* **91,** 7159-7163.

Reith, A. D., Rottapel, R., Giddens, E., Brady, C., Forrester, L. and Bernstein, A. (1990). *W* mutants mice with mild or severe developmental defects contain distinct point mutations in the kinase domain of the c-*kit* receptor. *Genes Dev.* **4,** 390-400.

Russell, E. S., Thompson, M. W. and McFarland, E. C. (1968). Analysis of effects of *W* and *f* genic substitutions on fetal mouse hematology. *Genetics* **58,** 259-270.

Sato, T. N., Towaza, Y., Deutsch, U., Wolburg-Buchlolz, K., Fujiwara, Y., Gendron-Maguire, M., Gridley, T., Wolburg, H., Risau, W. and Qin Y. (1995). Distinct roles of the receptor tyrosine kinases Tie-1 and Tie-2 in blood vessel formation. *Nature* **376,** 70-74.

Shalaby, F., Rossant, J., Yamaguchi, T. P., Gertsenstein, M., Wu, X.-F., Breitman, M. L. and Schuh, A. C. (1995). Failure of blood-island formation and vasculogenesis in Flk-1-deficient mice. *Nature* **376,** 62-66.

Thuneberg, L. (1982). Interstitial cells of Cajal: intestinal pacemakers? *Adv. Anat. Embryol. Cell Biol.* **71,** 1-130.

Tsukamoto, K., Jackson, I. and Hearing, V. (1992). DOPAchrome tautomerase: identification of its gene and catalytic activity. *EMBO J* **11,** 519-526.

Tsuzuki, T., Takahashi, M., Asai, N., Iwashita, T., Matsuyama, M. and Asai, J. (1995). Spatial and temporal expression of the *ret* proto-oncogene product in embryonic, infant and adult rat tissues. *Oncogene* **10,** 191-198.

Weiss, R. R., Whitakermenezes, D., Longley, J., Bender, J. and Murphy, G. F. (1995). Human dermal endothelial cells express membrane-associated mast cell growth factor. *J. Invest. Dermatol.* **104,** 101-106.

Witte, O. N. (1990) *Steel* locus defines new multipotent growth factor. *Cell* **63,** 5-6.

Yamaguchi, T. P., Dumont, D. J., Conlon, R. A., Breitman, M. L. and Rossant, J. (1993). *flk-1*, an *flt*-related receptor tyrosine kinase is an early marker for endothelial cell precursors. *Development* **118,** 489-498.

Young, P. E., Baumhueter, S. and Lasky, L. A. (1995). The sialomucin CD34 is expressed on hematopoietic cells and blood vessels during murine development. *Blood* **85,** 96-105.

Zambrowicz, B. P., Zimmermann, J. W., Harendza, C. J., Simpson, E. M., Page, D. C., Brinster, R. L. and Palmiter R. D. (1994). Expression of a mouse *Zfy-1/lacZ* transgene in the somatic cells of the embryonic gonad and germ cells of the adult testis. *Development* **120,** 1549-1559.

(Accepted 29 June 1996)